SUPPLEMENTARY APPENDIX

Deep sequencing and flow cytometric characterization of expanded effector memory CD8+CD57+ T cells frequently reveals T-cell receptor Vβ oligoclonality and CDR3 homology in acquired aplastic anemia

Valentina Giudice,[1] Xingmin Feng,[1] Zenghua Lin,[1,2] Wei Hu,[3] Fanmao Zhang,[3] Wangmin Qiao,[3] Maria del Pilar Fernandez Ibanez,[1] Olga Rios,[1] and Neal S. Young[1]

[1]Hematology Branch, National Heart, Lung, and Blood Institute (NHLBI), NIH, Bethesda, MD, USA; [2]Department of Hematology, Affiliated Hospital of Nantong University, Jiangsu, China and [3]BGI Genomics, BGI-Shenzhen, China

 doi:10.3324/haematol.2017.176701

Received: July 21, 2017.

Accepted: December 30, 2017.

Pre-published: February 1, 2018.

Correspondence: fengx2@nhlbi.nih.gov

Supplementary Methods

Human samples

Heparinized whole PB was collected from patients and healthy subjects after informed consent was obtained, in accordance with the Declaration of Helsinki[31] and protocols approved by the National Heart, Lung, and Blood Institute Institutional Review Board (National Institutes of Health, Bethesda, MD; Clinicaltrials.gov identifier: NCT00001620, NCT01623167, NCT00001397, NCT00071045, NCT00081523, NCT00961064) (*Online Supplementary Table S1* for clinical characteristics). HLA haplotypes were reported in *Online Supplementary Table S2*. All patients received a diagnosis of severe AA (SAA) according to the International Study of Aplastic Anemia and Agranulocytosis[32] and to the criteria of Camitta[33]. At the time of blood sampling, none of the patients had received therapy. Immunosuppressive therapies, such as cyclosporine A and anti-thymocyte globulin with or without eltrombopag, were administered according to protocols. Peripheral blood mononuclear cells (PBMCs) were isolated by Ficoll-Paque density gradient centrifugation (MP Biomedicals, LLC, Santa Ana, CA) according to the manufacturer's instructions.

Flow cytometric analysis

A minimum of $4x10^6$ PBMCs from each subject were stained for TCR Vβ repertoire analysis. Manufacturer's instructions of IOTest Beta Mark (Beckman Coulter, Miami, FL) were optimized as follows: 4 μL of Pacific Blue – conjugated anti-CD8, 5 μL of Brilliant Violet (BV) 510 – conjugated anti-CD28, 5 μL of BV605 – conjugated anti-CD3, 5 μL of allophycocyanin (APC) – conjugated anti-CD57, 5 μL of APC-phycoerythrin cytochrome 7 (Cy7) – conjugated anti-CD4 antibodies (all from BioLegend, San Diego, CA) were added. Cell mixture was divided into 8

individual tubes with different TCR Vβ antibody combinations (IOTest Beta Mark). After 20 min incubation at room temperature, samples were washed twice with phosphate buffered saline (PBS, Lonza, Walkersville, MD) and resuspended in the same buffer for acquisition. Expanded TCR Vβ clones found in IOTest Beta Mark kit were confirmed for accuracy with individual TCR Vβ antibodies (Beckman Coulter). Compensation was performed using single-color stained samples and an unstained sample as negative control. A LSR Fortessa cytometer equipped with FACSDiva software (v.8.0.1) (BD Biosciences, San Jose, CA) was used for acquisition, and FlowJo software (v.10.0.7b, Treestar, Ashland, OR) for analysis. Lymphocytes were identified based on forward and side scatter parameters and gated for CD3 expression. On $CD3^+$ population, $CD4^+$ and $CD8^+$ subsets were identified and gated for CD28 and CD57 expression. On $CD28^-CD57^+$ and $CD28^+CD57^-$ populations, each Vβ subfamily was studied (*Online Supplementary Figure S1*). Percentages of $CD28^+CD57^-$ and $CD58^-CD57^+$ cells were expressed as percent of $CD3^+CD8^+$ or $CD3^+CD4^+$ cells; similarly, each Vβ family size was expressed as percent of the given $CD4^+$ or $CD8^+$ cell population.

TCR repertoire deep sequencing

Before alignment, raw reads were filtered to remove reads containing adaptor sequences, false positive, and low-quality reads. For merging two paired-reads into one complete sequence, COPE software v1.1.3 (BGI, Cambridge, MA) was used for an overlap of $\geq$90% base matching (10 to 99 nucleotides [nt] for overlapped region). For other reads, FqMerger software (BGI) was used for 90% identity (matched bases) with overlap length of 50 to 150 nt. The alignment was performed by MiTCR software (milaboratory) using -pset flex -cysphe 1 -t 6 as parameters and by The International Immunogenetics Information System® (IMGT) as database

(http://www.imgt.org). The number of in-frame reads during analysis was counted as productive reads. The sequence included between the second conserved cysteine encoded by the 3' region of Vβ gene segment and the conserved phenylalanine encoded by the 5' portion of Jβ gene segment was considered as CDR3 β sequence[17].

Homology assessment

CDR3 amino acid sequences with frequency > 0.1% in $CD8^+$ cell pool were selected for homology analysis (Figure 6A) as previously described[17,40] to assess identical CDR3 sequences among filtered TCR repertoires.

Finally, immunodominant and shared CDR3 sequences were compared with CDR3 β repertoires reported in literature for cytomegalovirus[1-9], Epstein-Barr virus[3,6,9], BK virus[8], herpes-simplex virus type 1 and 2[10-12], varicella-Zoster virus[13], hepatitis C virus[14], and *Mycobacterium tuberculosis*[15-16] infections. Sequences from the following diseases were also analyzed: non-Hodgkin lymphomas[17], T-large granular lymphocyte leukemia (T-LGLL)[18], AA[19], paroxysmal nocturnal hemoglobinuria[20], juvenile dermatomyositis syndrome[21], multiple sclerosis[22], rheumatoid arthritis[23], systemic lupus erythematosus[24], cancers[25-30], Crohn's disease[31], and also from human mucosal-associated invariant T cell TCR repertoire[32].

Structural analysis of shared and immunodominant clonotypes was performed to identify similar charged residue pattern within CDR3 sequences, as described previously[8]. Amino acid sequences, as defined above, were aligned at N-terminal of Vβ and C-terminal of Jβ. ClustalW2 (https://www.ebi.ac.uk/Tools/msa/clustalw2/) was used to confirm our analysis.

Supplementary references

1. Suessmuth Y, Mukherjee R, Watkins B, et al. CMV reactivation drives post transplant T-cell reconstitution and results in defects in the underlying TCRβ repertoire. Blood. 2015;125(25):3835-3850.
2. Giest S, McWhinnie A, Lefranc MP, et al. Cytomegalovirus-specific CD8+ T cells targeting different peptide/HLA combinations demonstrate varying T-cell receptor diversity. Immunology. 2012;135(1):27-39.
3. Klarenbeek PL, Remmerswaal EB, ten Berge IJ, et al. Deep sequencing of antiviral T-cell responses to HCMV and EBV in humans reveals a stable repertoire that is maintained for many years. PLoS Pathog. 2012;8(9):e1002889.
4. Trautmann L, Rimbert M, Echasserieau K, et al. Selection of T cell clones expressing high-affinity public TCRs within Human cytomegalovirus-specific CD8 T cell responses. J Immunol. 2005;175(9):6123-6132.
5. Ruggiero E, Nicolay JP, Fronza R, et al. High-resolution analysis of the human T-cell receptor repertoire. Nat Commun. 2015;6:8081.
6. Venturi V, Chin HY, Asher TE, et al. TCR beta-chain sharing in human CD8+ T cell responses to cytomegalovirus and EBV. J Immunol. 2008;181(11):7853-7862.
7. Miconnet I, Marrau A, Farina A, et al. Large TCR diversity of virus-specific CD8 T cells provides the mechanistic basis for massive TCR renewal after antigen exposure. J Immunol. 2011;186(12):7039-7049.
8. Dziubianau M, Hecht J, Kuchenbecker L, et al. TCR repertoire analysis by next generation sequencing allows complex differential diagnosis of T cell-related pathology. Am J Transplant. 2013;13(11):2842-2854.

9. Lim A, Trautmann L, Peyrat MA, et al. Frequent contribution of T cell clonotypes with public TCR features to the chronic response against a dominant EBV-derived epitope: application to direct detection of their molecular imprint on the human peripheral T cell repertoire. J Immunol. 2000;165(4):2001-2011.
10. Held K, Eiglmeier I, Himmelein S, et al. Clonal expansions of $CD8^+$ T cells in latently HSV-1-infected human trigeminal ganglia. J Neurovirol. 2012;18(1):62-68.
11. Jing L, Laing KJ, Dong L, Russell RM, et al. Extensive CD4 and CD8 T Cell Cross-Reactivity between Alpha herpes viruses. J Immunol. 2016;196(5):2205-2218.
12. Dong L, Li P, Oenema T, McClurkan CL, Koelle DM. Public TCR use by herpes simplex virus-2-specific human CD8 CTLs. J Immunol. 2010;184(6):3063-3071.
13. D'Orsogna LJ, van Besouw NM, van der Meer-Prins EM, et al. Vaccine-induced allo-HLA-reactive memory T cells in a kidney transplantation candidate. Transplantation. 2011;91(6):645-651.
14. Meyer-Olson D, Shoukry NH, Brady KW, et al. Limited T cell receptor diversity of HCV-specific T cell responses is associated with CTL escape. J Exp Med. 2004;200(3):307-319.
15. Li D, Gao G, Li Z, et al. Profiling the T-cell receptor repertoire of patient with pleural tuberculosis by high-throughput sequencing. Immunol Lett. 2014;162(1 Pt A):170-180.
16. Luo W, Su J, Zhang XB, et al. Limited T cell receptor repertoire diversity in tuberculosis patients correlates with clinical severity. PLoS One. 2012;7(10):e48117.
17. Yin Q, Tan H, Chen S, Yang L, Ye J, Li Y. Characterization of conserved CDR3 sequence of TCR alpha- and beta-chain genes in peripheral blood T-cells from patients with diffuse large B-cell lymphoma. Hematology. 2010;15(1):48-57.

18. O'Keefe CL, Plasilova M, Wlodarski M, et al. Molecular analysis of TCR clonotypes in LGL: a clonal model for polyclonal responses. J Immunol. 2004;172(3):1960-1969.
19. Zeng W, Maciejewski JP, Chen G, Young NS. Limited heterogeneity of T cell receptor BV usage in aplastic anemia. J Clin Invest. 2001;108(5):765-773.
20. Gargiulo L, Lastraioli S, Cerruti G, et al. Highly homologous T-cell receptor beta sequences support a common target for autoreactive T cells in most patients with paroxysmal nocturnal hemoglobinuria. Blood. 2007;109(11):5036-5042.
21. Mizuno K, Yachie A, Nagaoki S, et al. Oligoclonal expansion of circulating and tissue-infiltrating CD8+ T cells with killer/effector phenotypes in juvenile dermatomyositis syndrome. Clin Exp Immunol. 2004;137(1):187-194.
22. Hong J, Zang YC, Tejada-Simon MV, et al. A common TCR V-D-J sequence in V beta 13.1 T cells recognizing an immunodominant peptide of myelin basic protein in multiple sclerosis. J Immunol. 1999;163(6):3530-3538.
23. Sun W, Nie H, Li N, et al. Skewed T-cell receptor BV14 and BV16 expression and shared CDR3 sequence and common sequence motifs in synovial T cells of rheumatoid arthritis. Genes Immun. 2005;6(3):248-261.
24. Sui W, Hou X, Zou G, et al. Composition and variation analysis of the TCR β-chain CDR3 repertoire in systemic lupus erythematosus using high-throughput sequencing. Mol Immunol. 2015;67(2 Pt B):455-464.
25. Vignard V, Lemercier B, Lim A, et al. Adoptive transfer of tumor-reactive Melan-A-specific CTL clones in melanoma patients is followed by increased frequencies of additional Melan-A-specific T cells. J Immunol. 2005;175(7):4797-4805.

26. Derré L, Bruyninx M, Baumgaertner P, et al. Distinct sets of alphabeta TCRs confer similar recognition of tumor antigen NY-ESO-1157-165 by interacting with its central Met/Trp residues. Proc Natl Acad Sci U S A. 2008;105(39):15010-15015.
27. Le Gal FA, Ayyoub M, Dutoit V, et al. Distinct structural TCR repertoires in naturally occurring versus vaccine-induced CD8+ T-cell responses to the tumor-specific antigen NY-ESO-1. J Immunother. 2005;28(3):252-257.
28. Serana F, Sottini A, Caimi L, et al. Identification of a public CDR3 motif and a biased utilization of T-cell receptor V beta and J beta chains in HLA-A2/Melan-A-specific T-cell clonotypes of melanoma patients. J Transl Med. 2009;7:21.
29. Wieckowski S, Baumgaertner P, Corthesy P, et al. Fine structural variations of alphabetaTCRs selected by vaccination with natural versus altered self-antigen in melanoma patients. J Immunol. 2009;183(8):5397-5406.
30. Dietrich PY, Le Gal FA, Dutoit V, et al. Prevalent role of TCR alpha-chain in the selection of the preimmune repertoire specific for a human tumor-associated self-antigen. J Immunol. 2003;170(10):5103-5109.
31. Chapman CG, Yamaguchi R, Tamura K, et al. Characterization of T-cell Receptor Repertoire in Inflamed Tissues of Patients with Crohn's Disease Through Deep Sequencing. Inflamm Bowel Dis. 2016;22(6):1275-1285.
32. Lepore M, Kalinichenko A, Colone A, et al. Parallel T-cell cloning and deep sequencing of human MAIT cells reveal stable oligoclonal TCRβ repertoire. Nat Commun. 2014;5:3866.

Supplementary Tables

Supplementary Table S1. Characteristics of patients and healthy donors.

Supplementary Table S2. SAA patients' (n=12) and healthy donors' (n=9) characteristics of TCR repertoire deep sequencing in $CD8^+$ T cells.

Supplementary Table S3. Frequency of PNH-related clonotypes.

Supplementary Table S1. Clinical characteristics.

	SAA (n=24)	PRCA (n=5)	MDS (n=8)	SCD (n=10)	Healthy controls (n=34)
Mean age (years)	38.7 (range, 7-79)	60.8 (range, 29-82)	60.4 (range, 38-79)	46.9 (range, 34-66)	41 (range 23-82)
Gender (M/F)	13/11	1/4	5/3	4/6	15/19
Transfusion history	23	5	6	10	-
No transfusion records	1	-	2	-	
CMV serostatus					
IgG positivity	15/24				
IgM positivity	1/24				
Median follow-up (months)	14.1 (range, 2.9-55.3)	-	-	-	-
Relapse/Death	7	-	-	-	-
Treatment		-	-	-	-
None	1				
CsA+ATG	3				
CsA+ATG+Eltrombopag	20				

SAA: severe acquired aplastic anemia; PRCA: pure red cell aplasia; MDS: myelodysplastic syndrome; SCD: sickle cell disease; CMV: cytomegalovirus; CsA: cyclosporine A; ATG: anti-thymocyte globulin.

Supplementary Table S2. SAA patients' (n=12) and healthy donors' (n=9) characteristics of TCR repertoire deep sequencing in $CD8^+$ T cells.

	CMV serostatus				HLA characterization							Deep sequencing				
	Age	**M/F**	**IgG (U/mL)**	**IgM (AU/mL)**	**A**	**A*02**	**B**	**C**	**DRB1**	**DQB1**	**DRB_**	**V gene**	**J gene**	**NGS frequency**	**Amino acid sequence**	**NGS frequency**
SAA patients (n=12)																
AA1	44	F	2.43	Neg.	02,30	01:01	14,44	05,08	01,04	03,05	4*01	TRBV2	TRBJ2-7	0.231	CASSVRDYEQYF	0.215
												TRBV20-1	TRBJ2-3	0.042	CSALPPGLASTDTQYF	0.022
												TRBV4-2	TRBJ1-2	0.041	CASSQEVGGTNYGYTF	0.040
AA2	71	M	2.52	Neg.	25,74		07,18	07,12	07,15	02,06	4*01	TRBV15	TRBJ2-5	0.349	CATSTGTWTEQETQYF	0.346
											5*01	TRBV7-9	TRBJ2-7	0.139	CASSFRDWGRYEQYF	0.128
												TRBV20-1	TRBJ2-7	0.097	CSARDLAEEQYF	0.093
AA3	59	F	Neg.	Neg.	01,02	01	07,18	07,07	04,11	03,03	3*02	TRBV20-1	TRBJ2-3	0.541	CSARDPPVSGTRGTDTQYF	0.536
						246					4*01	TRBV6-6	TRBJ2-1	0.024	CASSYRETNEQFF	0.023
						338						TRBV15	TRBJ2-7	0.021	CATSRETGAAEQYF	0.018
AA4	44	M	>5.0	Neg.	02,74	01:01	35,57	07,16	08,13	02,03	3*02	TRBV15	TRBJ2-1	0.240	CATSSSRSGQGLNEQFF	0.234
						90						TRBV15	TRBJ1-1	0.147	CATSRPFPGQGAN*AEAFF	0.142
						195						TRBV24-1	TRBJ2-7	0.054	CATSDPLTASYEQYF	0.049
AA5	55	M	>5.0	Neg.	33,36	.	45,58	03,16	03,12	02,03	3*02	TRBV9	TRBJ2-2	0.162	CASGGANSPLHF	0.119
												TRBV20-1	TRBJ2-6	0.050	CSAPDDGANVLTF	0.047
												TRBV29-1	TRBJ2-7	0.027	CSVEADNRAGANVLTF	0.000
AA6	30	M	2.53	Neg.	02,33	02	40,53	03,04	04,15	03,06	4*01	TRBV5-6	TRBJ2-1	0.176	CASSLD~SNEQFF	0.176
											5*01:01	TRBV6-4	TRBJ2-5	0.118	CASSEGLESETQYF	0.113
												TRBV20-1	TRBJ2-1	0.111	CSAPGSGDRNEQFF	0.103
AA7	49	M	Neg.	Neg.	01,26		07,27	06,07	11,15	03,06	3*02	TRBV12-4, 12-3	TRBJ2-2	0.043	CASSFTGELFF	0.041
											5*01:01	TRBV15	TRBJ1-1	0.039	CATGSTRTGGRTEAFF	0.036
												TRBV5-6	TRBJ1-2	0.035	CASSLAGNYGYTF	0.030
AA8	40	F	Neg.	Neg.	03,24		07,49	07,07	11,15	03,06	3*02	TRBV20-1	TRBJ2-7	0.034	CSARDAADYEQYF	0.008
											5*01:01	TRBV20-1	TRBJ1-1	0.030	CSASRAGGVTEAFF	0.009
												TRBV20-1	TRBJ2-6	0.027	CSARDAP~GANVLTF	0.015
AA9	55	F	> 10	Neg	11,26		51,52	07,12	04,10	03,05	4*01	TRBV20-1	TRBJ1-5	0.193	CSATDG~NQPQHF	0.189
												TRBV15	TRBJ2-5	0.221	CATSRVAGETQYF	0.188
												TRBV7-8	TRBJ2-7	0.075	CASSSPGQFDEQYF	0.072
AA10	57	F	> 10	Neg	11,29		07,14	08,15	11,15	03,06	3*02	TRBV7-8	TRBJ2-3	0.117	CASSLAGGPDTQYF	0.116
											5*01	TRBV2	TRBJ2-3	0.086	CASGDGGTDTQYF	0.083

												TRBV11-3	TRBJ1-1	0.043	CASSLDLTGNTEAFF	0.042
AA11	16	M	7.2	Neg	02,30		07,57	07,18	11,15	03,06	3*02	TRBV10-3	TRBJ2-5	0.033	CAISESSFSSQETQYF	0.028
											5*01:01	TRBV10-2	TRBJ1-2	0.026	CASSESRGYNYGYTF	0.024
												TRBV4-3	TRBJ1-6	0.019	CASSQDLLPGDNSPLHF	0.018
AA12	14	M	2.6	Neg	24		07,52	03,07	14,15	03,06	3*01	TRBV5-1	TRBJ1-2	0.064	CASSQR~GGYTF	0.061
											5*01:01	TRBV10-1	TRBJ2-7	0.022	CASSDGGPSYEQYF	0.020
												TRBV3-1	TRBJ2-7	0.011	CASSPRQGVDEQYF	0.010
Healthy controls (n=9)																
HC1	35	M										TRBV15	TRBJ2-1	0.107	CATSRDGDLGYNEQFF	0.101
												TRBV5-6	TRBJ2-7	0.094	CASSLDPGSYEQYF	0.091
												TRBV24-1	TRBJ1-5	0.069	CATSLAG~DQPQHF	0.065
HC2	36	M										TRBV12-4, 12-3	TRBJ1-2	0.092	CASSSANYGYTF	0.088
												TRBV20-1	TRBJ2-7	0.059	CSAPGGGGQGNPEQYF	0.016
												TRBV4-1	TRBJ1-1	0.056	CASSQEQTDANTEAFF	0.055
HC3												TRBV7-9	TRBJ2-2	0.121	CASSLDSPPFGELFF	0.119
												TRBV29-1	TRBJ2-7	0.091	CSVEGGSSYEQYF	0.045
												TRBV6-1	TRBJ2-7	0.068	CASMDWGQDRAYEQYF	0.066
HC4	38	F										TRBV10-3	TRBJ1-6	0.051	CAISELWARPVGNSPLHF	0.049
												TRBV10-2	TRBJ2-5	0.041	CASQGTGEKTQYF	0.041
												TRBV10-1	TRBJ1-1	0.016	CASSERKG~GGSTEAFF	0.016
HC5	27	F										TRBV25-1	TRBJ2-7	0.150	CASSGGGRGIKNEQYF	0.132
												TRBV5-1	TRBJ2-3	0.072	CASSLEGGYTDTQYF	0.066
												TRBV20-1	TRBJ2-7	0.037	CSAIPTGTYEQYF	0.019
HC6	28	F										TRBV25-1	TRBJ2-3	0.383	CASSALAGAGDTQYF	0.379
												TRBV10-1	TRBJ2-2	0.191	CASTID~GELFF	0.190
												TRBV6-4	TRBJ1-6	0.036	CASSDSSGGNSPLHF	0.036
HC7	23	M										TRBV7-9	TRBJ2-1	0.089	CASSLAERLSSYNEQFF	0.084
												TRBV19	TRBJ2-5	0.072	CASSTWDRGSRETQYF	0.052
												TRBV29-1	TRBJ1-2	0.043	CSAVRQGEYGYTF	0.041
HC8	24	F										TRBV19	TRBJ1-1	0.032	CASSIVGRGDTEAFF	0.020
												TRBV20-1	TRBJ2-5	0.030	CSASGASGELRETQYF	0.018
												TRBV29-1	TRBJ2-5	0.017	CSVEVSWTGG*ETQYF	0.013
HC9	32	F										TRBV7-6	TRBJ2-5	0.533	CASSLGETQYF	0.056
												TRBV20-1	TRBJ2-1	0.0003	CSSGPYNEQFF	0.027
												TRBV7-7	TRBJ2-7	0.0002	CASSLAPGSTYEQYF	0.026

SAA: severe acquired aplastic anemia; TCR: T-cell receptor; CMV: cytomegalovirus; HLA: human leukocyte antigen; NGS: next-generation sequencing.

Supplementary Table S3. Frequency of PNH-associated clonotypes.

	CASSLVGGPEQYF	CATSRVAGETQYF	CATSRTAGETQYF	CATSRTGGETQYF	CATSRVGGETQYF	CATSRDLAGETQYF
AA1				0.0001		
AA2				0.0456		
AA3	0.00002			0.0001		
AA4	0.00001			0.0003		
AA5						
AA6				0.0003		
AA7				0.0002		
AA8	0.00003			0.0002		
AA9		18.8384	0.00003	0.6668	9.7E-05	1.4E-05
AA10		0.0105		0.0004		
AA11		0.0115		0.0003		
AA12		0.0170		0.0006		
AA3 CD57						
AA4 CD57						
HC1	0.00002			0.0002		
HC2	0.00001			0.0002		
HC3				0.0002		
HC4		0.0090		0.0003		
HC5		0.0127		0.0005		
HC6		0.0083		0.0003		2.2E-03
HC7		0.0104		0.0004		
HC8		0.0102		0.0003		
HC9						

PNH: paroxysmal nocturnal hemoglobinuria; AA: acquired aplastic anemia patient identification number; HC: healthy control identification number. PNH-related CDR3 sequences are from *Gargiulo L, et al. Blood. 2007;109(11):5036-5042.*

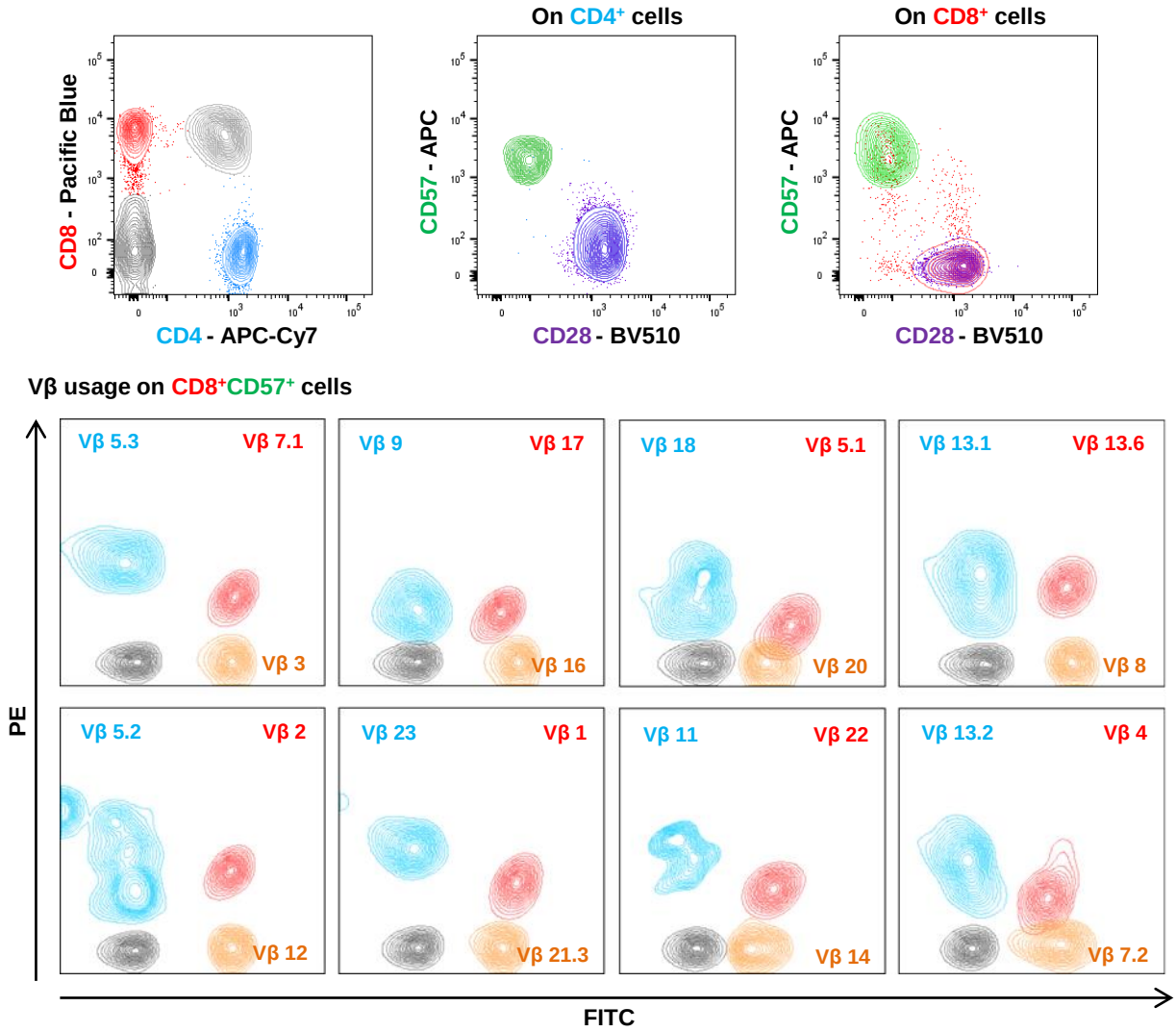

Supplementary Figure S1. Vβ usage in CD4⁺ and CD8⁺ subsets.
CD28⁺ and CD57⁺ subsets were gated on CD4⁺ and CD8⁺ T cells respectively (top panels) and, on each population, Vβ usage was studied (bottom panels) using a double immunofluorescence (FITC/PE) staining with 8 different Vβ mAbs mixtures in combination with CD3 - BV605, CD4 – APC-Cy7, CD8 – Pacific Blue, CD28 – BV510, and CD57 – APC.

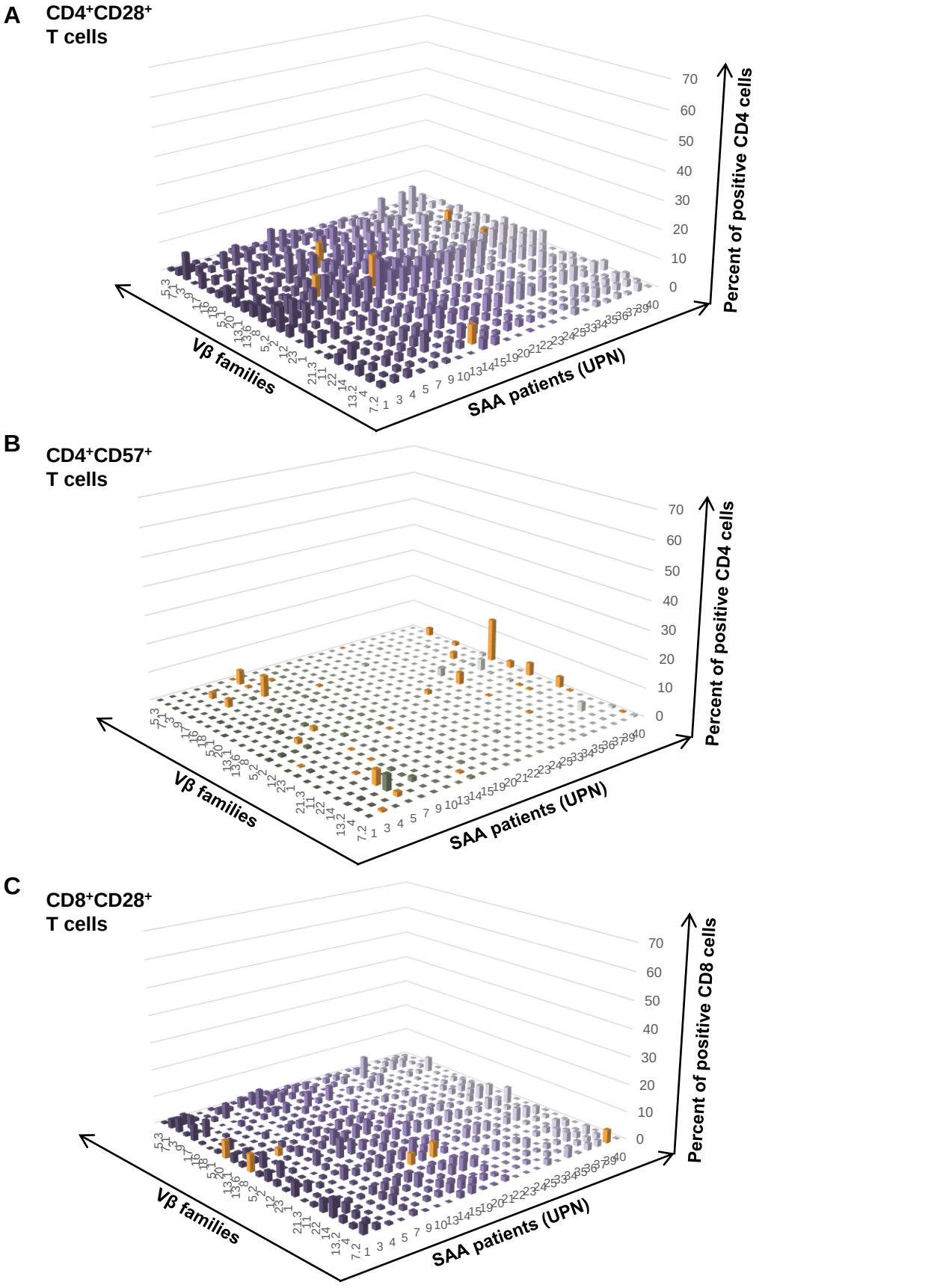

Supplementary Figure S2. Vβ usage of different T cell compartments in SAA patients.

Vβ usage was studied in $CD4^+CD28^+$ (A), $CD4^+CD57^+$ (B), and $CD8^+CD28^+$ (C) T cells. A bar graph was made for each SAA patient, as described in Figure 2 A.

Supplementary Figure S3. Giudice V. et al.

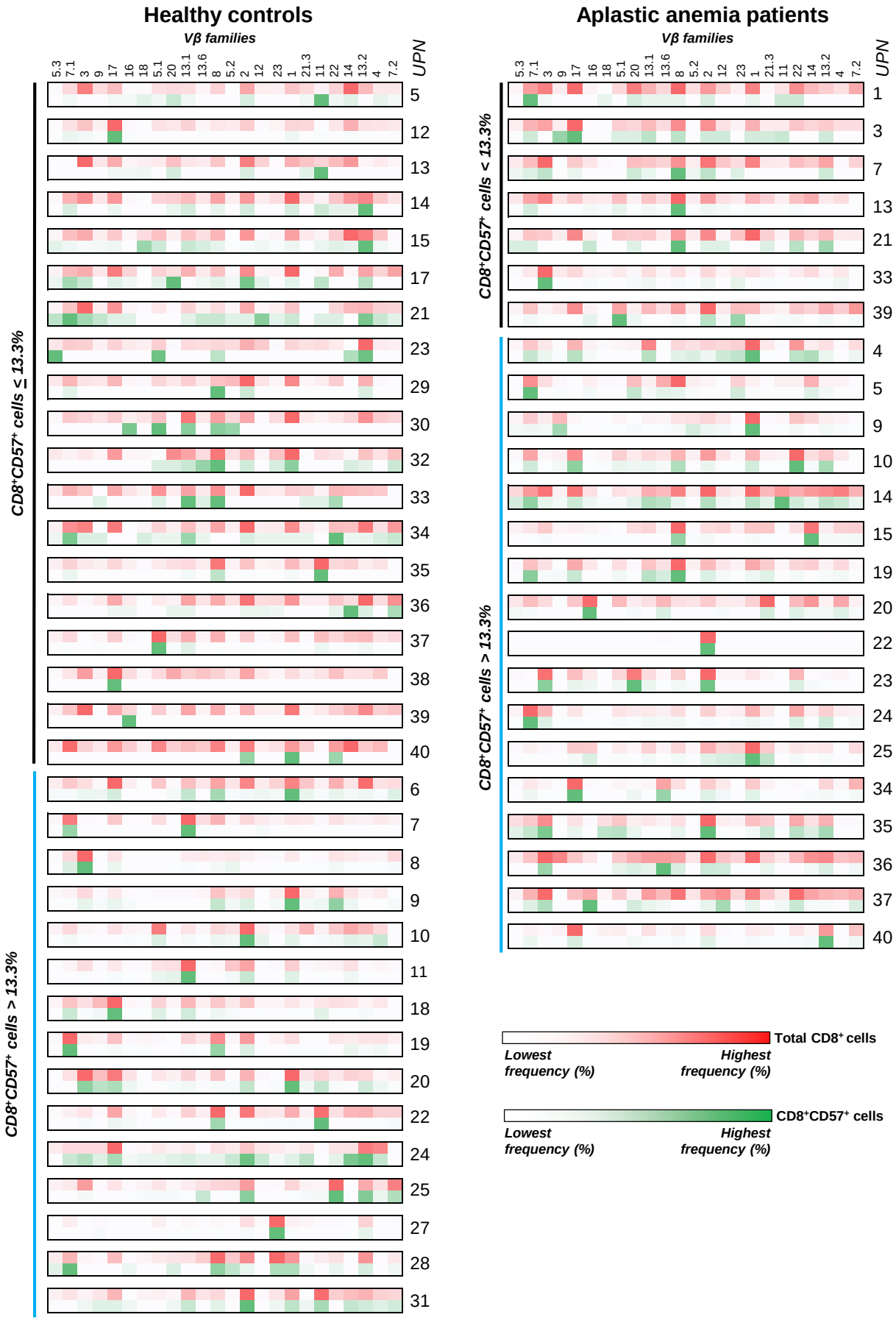

Supplementary Figure S3. Vβ usage analysis in total $CD8^+$ and effector memory $CD8^+$ cells by flow cytometry.

Vβ usage was studied in $CD8^+CD57^+$ and total $CD8^+$ cells for each healthy donor and SAA patient. Subjects (UPN) were divided using the mean frequency of $CD8^+CD57^+$ cells in healthy donors (13.3%) as a cut-off. Results were plotted as relative frequency and converted in color scale. For Vβ usage in effector memory $CD8^+$ cells (bottom row in each subject), colors range from white to green (from 0% to highest value); while, for total $CD8^+$ cells (top row in each subject), colors range from white to red (from 0% to highest value).

Supplementary Figure S4. Giudice V. et al.

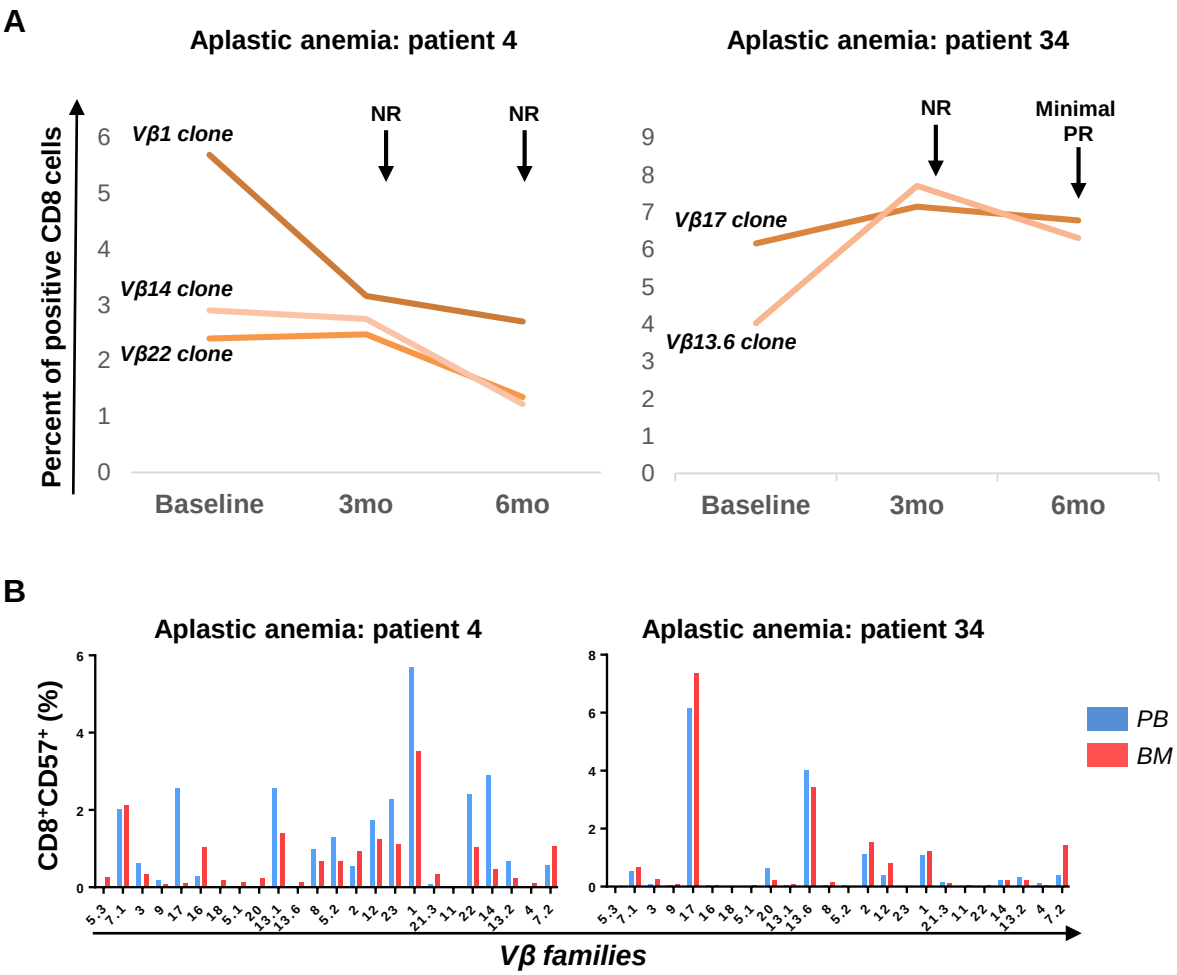

Supplementary Figure S4. Vβ usage analysis in effector memory CD8$^+$ cells by flow cytometry during the course of disease and in peripheral blood (PB) and bone marrow (BM).

(A) Vβ usage was studied in CD8$^+$CD57$^+$ cells from PB of two patients at 3 (3mo) and 6 months (6mo) of immunosuppressive therapies. Both patients were non-responders (NR) at 3 months. At 6 month timepoint, patient 4 was NR, while patient 34 achieved a minimal partial-response (PR). (B) Vβ usage was compared between PB and BM at baseline for these two SAA patients and results shown as bar graphs.

Supplementary Figure S5. Giudice V. et al.

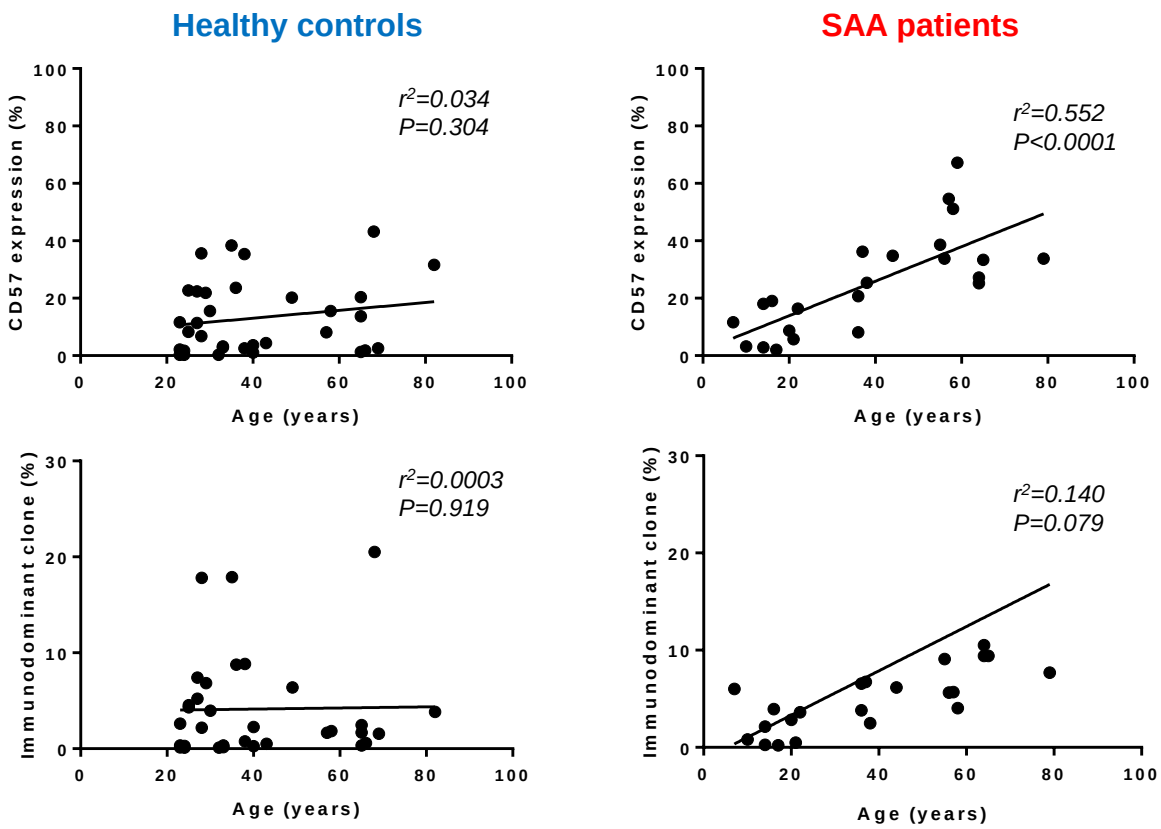

Supplementary Figure S5. Age-effects assessment on CD57 expression and clone size.

Linear regression analysis was performed to exclude age-effects on CD57 expression (top) and clone size (bottom). The percentage of the immunodominant clones (bottom panels) were calculated on $CD8^+CD57^+$ cells as total $CD8^+$ cell percentage. R square and p values were reported. $P<0.05$ was considered statistically significant.

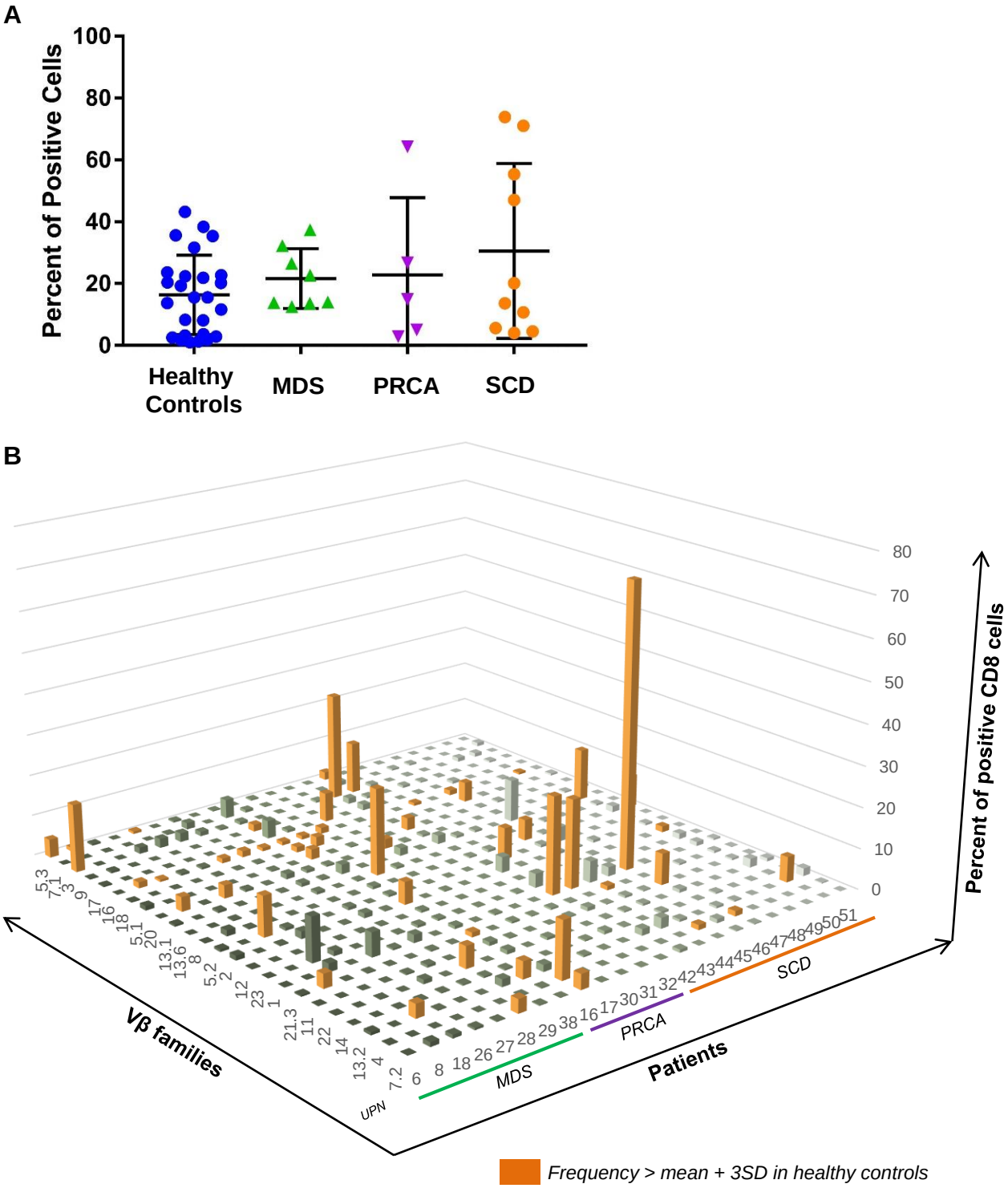

Supplementary Figure S6. Frequency of CD8$^+$CD57$^+$ cells and Vβ usage analysis in other hematological diseases.

(A) Percentages of CD8$^+$CD57$^+$ cells were calculated on CD8$^+$ compartment for healthy controls, myelodysplastic syndrome (MDS), pure red cell aplasia (PRCA) and sickle cell disease (SCD) patients. Data are shown as mean±SD. Unpaired t-test was performed and $P<0.05$ was considered statistically significant. (B) Percentages of Vβ family in CD8$^+$CD57$^+$ cells were calculated on total CD8$^+$ cells, and Vβ skewing in patients was defined using the mean+3SD of a given Vβ group in healthy donors. Relative expansion of each Vβ subgroup is shown in the bar graph. Patients were divided based on the disease. The skewing of one Vβ family is reported as orange bar.

Supplementary Figure S7. Giudice V. et al.

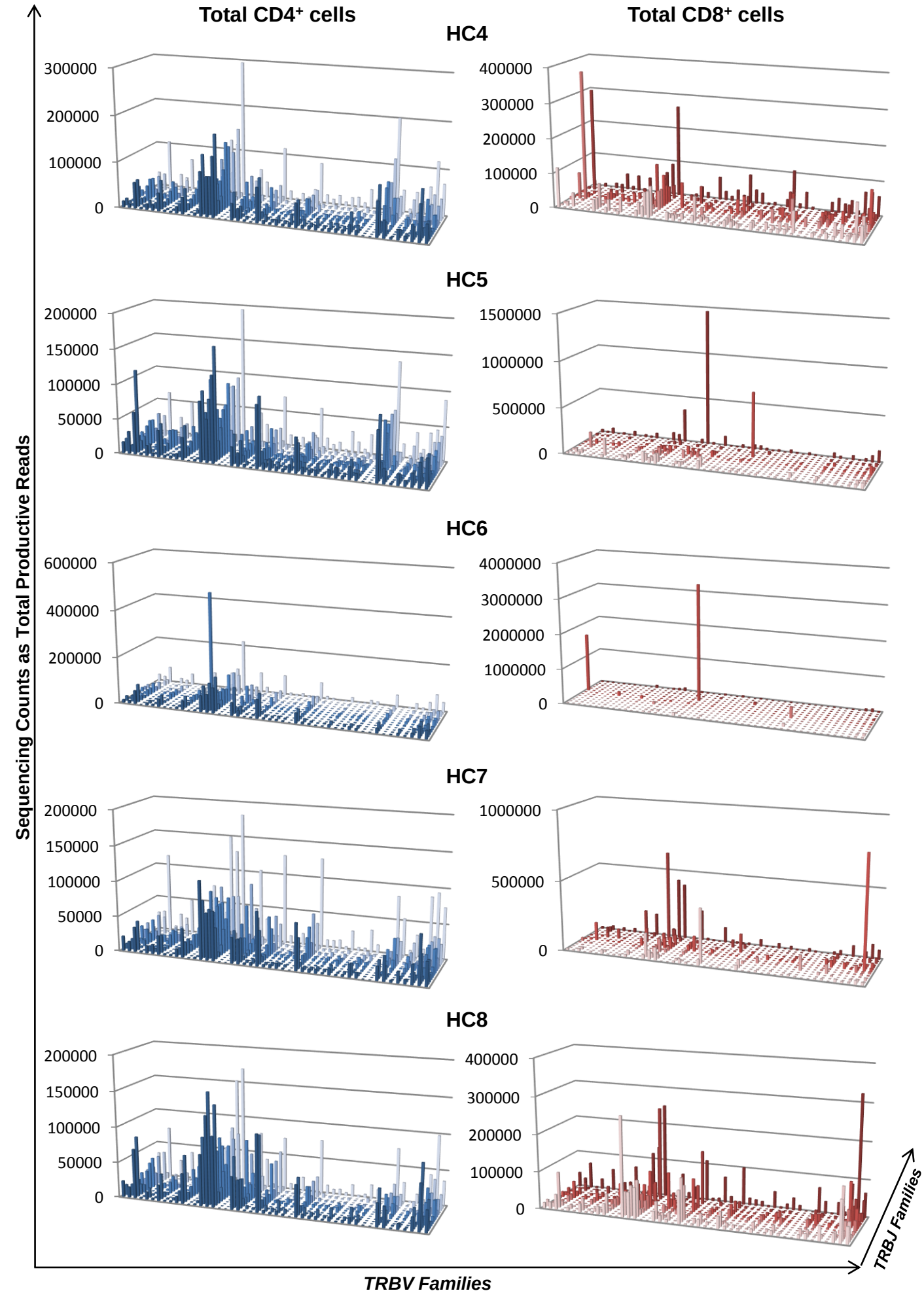

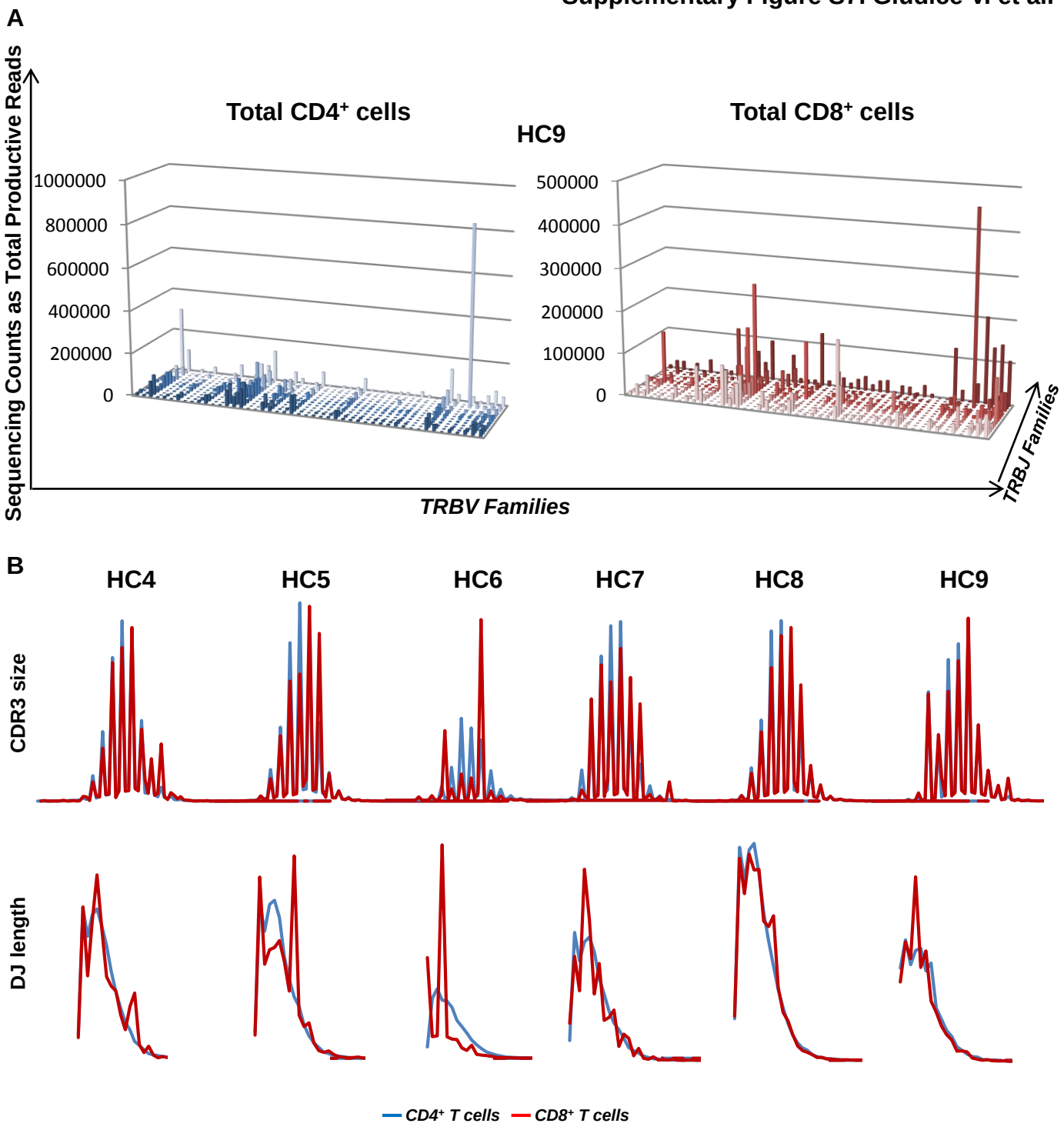

Supplementary Figure S7. Characterization of Vβ/Jβ plot, CDR3 size and DJ length profiles in healthy donors by deep sequencing.
(A) T-cell receptor beta variable (TRBV)/T-cell receptor beta joining (TRBJ) plots showed citylike landscape for total $CD4^+$ and $CD8^+$ cell populations in healthy subjects (HC). (B) The complementarity region 3 (CDR3) size and DJ length profiles also were defined, showing similar features in $CD4^+$ and $CD8^+$ cells.

Supplementary Figure S8. Giudice V. et al.

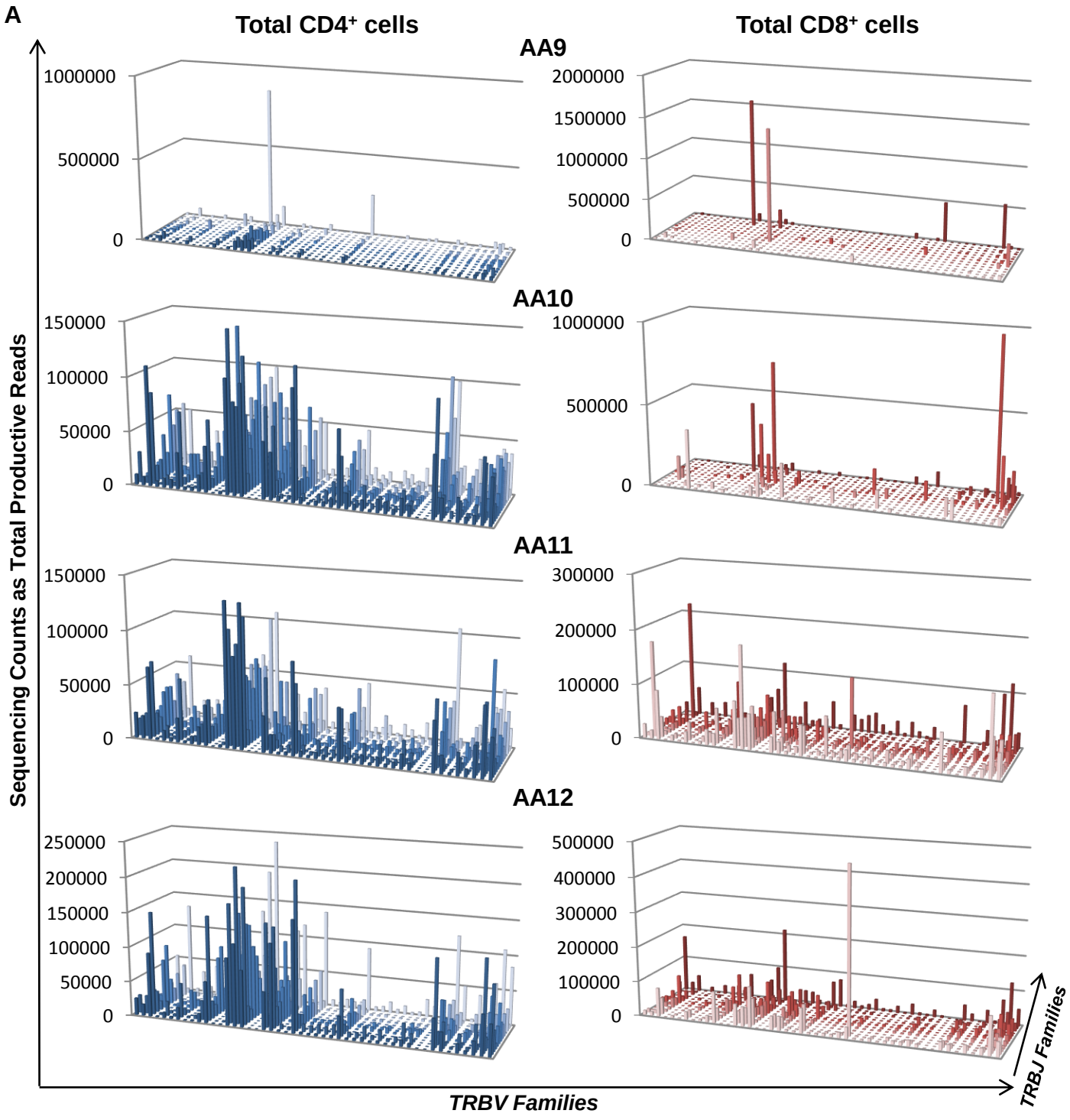

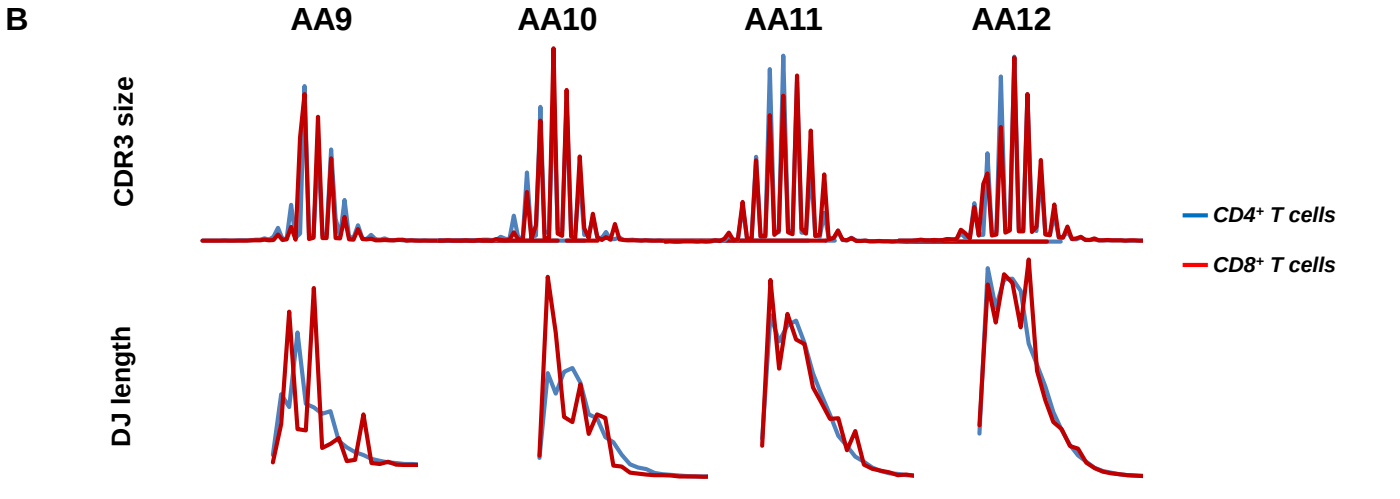

Supplementary Figure S8. Characterization of Vβ/Jβ plot, CDR3 size and DJ length profiles in severe aplastic anemia patients by deep sequencing.

(A) T-cell receptor beta variable (TRBV)/T-cell receptor beta joining (TRBJ) plots showed citylike landscape for total $CD4^+$ cells, and oligoclonality in $CD8^+$ cell population in aplastic anemia (AA) subjects. (B) The complementarity region 3 (CDR3) size and DJ length profiles also were defined in $CD4^+$ and $CD8^+$ cells.

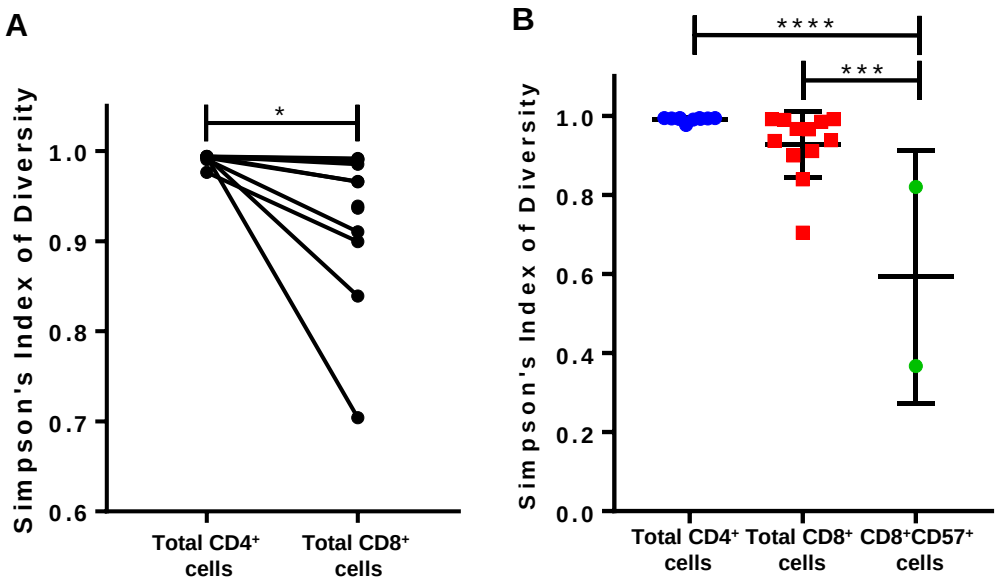

Supplementary Figure S9. Simpson's index of diversity in aplastic anemia patients.

(A) By paired t-test, Simpson's indexes were compared between total $CD4^+$ and total $CD8^+$ cells for each AA patient. (B) Simpson's indexes were calculated for each patient in total $CD4^+$, $CD8^+$ and $CD8^+CD57^+$ cell populations, and compared by one-way ANOVA with Turkey's multiple comparison test. *, $P<0.05$; ***, $P<0.001$; ****, $P<0.0001$.